Bridging the Gap Between Target Networks and Functional Regularization

Alexandre Piché* Mila, Université de Montréal ServiceNow Research

Valentin Thomas* Mila, Université de Montréal

Joseph Marino DeepMind

Rafael Pardiñas ServiceNow Research

Gian Maria Marconi RIKEN

Christopher Pal Mila, Polytechnique Montréal Canada CIFAR AI Chair

Mohammad Emtiyaz Khan RIKEN

Abstract

Bootstrapping is behind much of the successes of Deep Reinforcement Learning. However, learning the value function via bootstrapping often leads to unstable training due to fast-changing target values. Target Networks are employed to stabilize training by using an additional set of lagging parameters to estimate the target values. Despite the popularity of Target Networks, their effect on the optimization is still misunderstood. In this work, we show that they act as an implicit regularizer. This regularizer has disadvantages such as being inflexible and non convex. To overcome these issues, we propose an explicit Functional Regularization that is a convex regularizer in function space and can easily be tuned. We analyze the convergence of our method theoretically and empirically demonstrate that replacing Target Networks with the more theoretically grounded Functional Regularization approach leads to better sample efficiency and performance improvements.

1 Introduction

Value functions are at the core of deep Reinforcement Learning (RL) algorithms. In order to learn a value function via regression, we need to estimate the target value of the state. Estimating the target value using Monte Carlo roll-outs requires complete trajectories and can have high variance. These issues make value estimation via Monte Carlo inefficient and unpractical in complex environments. Temporal Difference (TD) (Sutton, 1988) algorithm addresses these issues by using *bootstrapping* (Sutton and Barto, 2018). Specifically, the value of a state is estimated using the immediate reward and the discounted predicted value of its successor. Bootstrapping has potentially lower variance than Monte Carlo, particularly in the off-policy settings, and does not require entire trajectories to estimate the target value. Bootstrapping can unfortunately be unstable as the target value is estimated with constantly updated parameters.

To stabilize value function training, Mnih et al. (2013) proposed using *Target Networks* (TN): an additional set of lagging parameters to estimate the target value. Today TNs are central to most modern deep RL algorithms (Mnih et al., 2013; Lillicrap et al., 2015; Abdolmaleki et al., 2018b; Haarnoja et al., 2018; Fujimoto et al., 2018; Hausknecht and Stone, 2015; Van Hasselt et al., 2016; Hessel et al., 2018). Their popularity is due to the ease of implementation, no computation overhead, and their demonstrated effectiveness in a range of domains. Despite their popularity, the inner workings of TNs and how they stabilize the optimization of the value function remain unclear. While Van Hasselt et al. (2018) empirically shows that TNs help but do not prevent divergence, Zhang et al. (2021) shows that a variant of TNs can prevent divergence in simple cases.

In this work, we shed light on the regularization implicitly performed by TNs and how it is related to a regularization in the Q-function space whose strength is dictated by the discount factor γ. However, this regularization cannot be written as the gradient of a convex regularizer, as is commonplace in optimization. We prove that, because of this, TNs can unstabilize TD instead of making it more stable. This leads us to propose a simple Functional Regularization (FR) alternative that has the advantages of provably ensuring TD remains stable while being more flexible than TN.

Preprint.

We then empirically confirm our theoretical results. We first compare the stability of TN and FR on a simple two-state MDP (Tsitsiklis and Van Roy, 1996). Then, in the Four Rooms environment (Sutton et al., 1999), we find that when combined with Deep Neural Networks (DNNs), the added flexibility of FR results in better performance, especially when learning with off-policy data. Finally, on the Atari suite (Bellemare et al., 2013), we demonstrate that replacing TN with FR on 3 popular algorithms leads to performance gains.

2 Background

Preliminaries. We consider the general case of a Markov Decision Process (MDP) (Puterman, 2014) defined by $\{\mathcal{S}, \mathcal{A}, p, r, \gamma, \mu\}$, where $\mathcal{S}$ and $\mathcal{A}$ respectively denote the finite state and action spaces, $p(\mathbf{s}'|\mathbf{s}, \mathbf{a})$ represents the environment transition dynamics, i.e the distribution of the next state taking action $\mathbf{a}$ in state $\mathbf{s}$. $r\colon \mathcal{S} \times \mathcal{A} \to \mathbb{R}$ denotes the reward function, $\gamma \in [0, 1)$ is the discount factor, and μ is the initial state distribution. For a given policy, $\pi : \mathcal{S} \to \Delta(\mathcal{A})$, a starting state $\mathbf{s}$ and action $\mathbf{a}$, the value function $Q^\pi \in \mathbb{R}^{|\mathcal{S}|\times|\mathcal{A}|}$ is the expected discounted sum of rewards:

$$Q^\pi(\mathbf{s}, \mathbf{a}) = \mathbb{E}_\pi\left[\sum_{t\geq 0} \gamma^r r(\mathbf{s}_t, \mathbf{a}_t)|\mathbf{s}_0 = \mathbf{s}, \mathbf{a}_0 = \mathbf{a}\right]. \quad (1)$$

Additionally, the value function satisfies the Bellman equation (Bellman, 1966)

$$Q^\pi = R + \gamma P^\pi Q^\pi \equiv \mathcal{T}Q^\pi \quad (2)$$

where $R \in \mathbb{R}^{|S|\cdot|A|}$ the reward vector and the state-action to state-action transition matrix $P^\pi \in \mathbb{R}^{|\mathcal{S}|\cdot|\mathcal{A}|\times|\mathcal{S}|\cdot|\mathcal{A}|}$ where $P^\pi\big[(\mathbf{s}, \mathbf{a}), (\mathbf{s}', \mathbf{a}')\big] = \pi(\mathbf{a}'|\mathbf{s}') \cdot p(\mathbf{s}'|\mathbf{s}, \mathbf{a})$ and $\mathcal{T} : \mathbb{R}^{|\mathcal{S}|\cdot|\mathcal{A}|\times|\mathcal{S}|\cdot|\mathcal{A}|} \to \mathbb{R}^{|\mathcal{S}|\cdot|\mathcal{A}|\times|\mathcal{S}|\cdot|\mathcal{A}|}$ is the Bellman operator.

Linear Function Approximation (LFA). The value function Q^π can be approximated via a linear function. For a fixed feature matrix $\Phi \in \mathbb{R}^{|S|\cdot|A|\times p}$, our aim is to learn a parameter vector of dimension p, $w \in \mathbb{R}^p$, so that $Q_w \equiv \Phi w$ approximates Q^π. We denote the the off-policy sampling distribution by the diagonal matrix $D \in \mathbb{R}^{|S|\cdot|A|\times|S|\cdot|A|}$ with diagonal entries $d(s, a)$, positive and summing to 1. The update rule given by the TD(0) semi-gradient (Sutton and Barto, 2018) is given by

$$\nabla_w \ell^{\text{TD}}(w) = -\Phi^\top D(R + \gamma P^\pi \Phi w - \Phi w) \quad (3)$$

where the remainder of the return is estimated via bootstrapping, i.e., $P^\pi \Phi w$.

Deep Neural Networks (DNNs) Approximation. In complex environments, linear functions can result in a poor approximation of Q^π. Instead, non-linear functions, such as DNNs, are used to parametrize Q_w and improve the approximation to Q^π. But using DNNs to estimate Q^π using off-policy data and bootstrapping can be unstable and diverge (Sutton and Barto, 2018; Van Hasselt et al., 2018). It is common to use a lagging set of weights $\bar{w}$ to estimate the next value function to mitigate divergence (Mnih et al., 2013; Lillicrap et al., 2015). The network parametrized by the set of lagging weights is commonly referred to as a target network. Despite the popularity of target networks, there are still gaps in our understanding of the impact it has on learning dynamics.

3 Functional Regularization for stable Reinforcement Learning

3.1 Understanding Target Network's implicit regularization

In this subsection, we will look more closely at the effects TNs have on the optimization. We place ourselves in the classical Linear Function Approximation (LFA) setting (Sutton and Barto, 2018) in order to be able to make theoretical contributions.

Target Networks (Mnih et al., 2013) are a popular approach to stabilize Temporal Difference learning. A periodically updated copy, $Q_{\bar{w}}$, of Q_w is used to estimate the next state value. This causes the regression targets to no longer directly depend on the most recent estimate of w. With this, the Mean Squared Bellman Error for a given state transition is

$$\ell^{\text{TN}} = \|R + \gamma P^\pi Q_{\bar{w}} - Q_w\|_D^2. \quad (4)$$

The semi-gradient (Sutton and Barto, 2018) of the expected squared Bellman error with a TN can be decomposed as (see proof in Appendix A)

$$\nabla_w \ell^{\text{TN}}(w) = \underbrace{-\Phi^\top D(R + \gamma P^\pi \Phi w - \Phi w)}_{\text{TD(0)}} + \underbrace{\gamma\, \Phi^\top D P^\pi \Phi(w - \bar{w})}_{\text{“}Regularizer\text{”}}. \quad (5)$$

Written in this form, the effects of using TNs become clearer. The first term is the usual TD(0) update that we will not attempt to modify in this paper, and the second term can be interpreted as a "regularization" term that encourages the weights w to stay close to the frozen weights $\bar{w}$. This is in line with the intuition that TNs "slow down" or "stabilize" the optimization. However, this "regularizer" suffers from two main issues.

- The first one is the weighting of the regularization which is equal to the discount factor γ. This may be problematic as γ controls the agent's effective horizon (Sutton and Barto, 2018) and is part of the problem definition. Therefore TNs are inflexible in the

sense that the weight of the regularizer cannot be controlled independently from the agent's effective horizon, and can only be controlled through the target update period T. We show experimentally in Section 4.2 that the update period T can be ineffective at controlling the strength of the regularization.

- The second and most important point is that the "regularization" is not a proper regularization term. It may be interpreted as the gradient of a quadratic when $\Phi^\top D P^\pi \Phi$ is symmetric and positive, which is not the case in general. The underlying issue is that if $\Phi^\top D P^\pi \Phi$ has a negative eigenvalue, the "regularizer" will actually push w away from $\bar{w}$ instead of bringing them closer and thus will render the whole optimization unstable. **This is an important theoretical issue as usually a basic requirement for a regularizer is that it cannot cause the original method to diverge.** It is verified in Section 4.1 that TN can create additional divergence zones that were not present in TD(0).

Both aforementioned issues can be resolved simply. For the first point, we replace γ by a separate hyper-parameter $\kappa \geq 0$. As for the second point, changing $\Phi^\top D P^\pi \Phi$ to $\Phi^\top D \Phi$ ensures that the second term is a proper quadratic regularizer that cannot destabilize the optimization (Tihonov, 1963; Tikhonov, 1943; Lyapunov, 1992).

3.2 Introducing Functional Regularization

Following the reasoning developed in the previous subsection, we would like to design a loss ℓ whose semi-gradient is

$$\nabla_w \ell(w) = \Phi^\top D(R + \gamma P^\pi \Phi w - \Phi w) + \kappa\, \Phi^\top D \Phi (w - \bar{w}). \tag{6}$$

The term $\kappa\, \Phi^\top D \Phi (w - \bar{w})$ is the gradient of the quadratic form

$$\frac{\kappa}{2}(w - \bar{w})^\top \Phi^\top D \Phi (w - \bar{w}) = \frac{\kappa}{2} \|Q_w - Q_{\bar{w}}\|_D^2$$

as $Q_w = \Phi w$. We see that the natural resulting regularizer is a Functional Regularizer in norm $\|\cdot\|_D$, the usual norm when studying the convergence of TD in RL (Bertsekas and Tsitsiklis, 1996). This leads to the *Functionally regularized* Mean Square Bellman Error which penalizes the norm between the current Q-value estimate $Q_w(\mathbf{s}, \mathbf{a})$ and a lagging version of it $Q_{\bar{w}}(\mathbf{s}, \mathbf{a})$, giving us

$$\ell^{\text{FR}}(w) = \frac{1}{2}\|R + \gamma P^\pi Q_w - Q_w\|_D^2 + \frac{\kappa}{2}\|Q_w - Q_{\bar{w}}\|_D^2 \tag{7}$$

We observe that the up-to-date parameter w is used in the Squared Bellman Error and there is the additional decoupled FR loss to stabilize w by regularizing the Q function. $\kappa \geq 0$ is the regularization parameter and we recover TD learning for $\kappa = 0$.

Critically, unlike Equation (4), the target Q-value estimates are supplied by the up-to-date Q-network, with the explicit regularization now separately serving to stabilize training. As with a TN, we can update the lagging network periodically to control the stability of the Q-value estimates. Overall, ℓ^{FR} is arguably similar in complexity to ℓ^{TN}, requiring only an additional function evaluation for $Q_w(\mathbf{s}_{t+1}, \mathbf{a}_{t+1})$ and an additional hyper-parameter, κ.

3.3 Stability of Target Network regularization and Functional Regularization

Now that we have highlighted potential issues that could arise when using TNs and proposed an alternative objective function, we will show that indeed TN can *unstabilize* Temporal Difference learning while FR, under some conditions, does not.

Theorem 3.1 (Target Networks can **unstabilize** TD)**.** *Using TD(0) with Target Networks (Equation* (4)*) can diverge while using TD(0) only would converge.*

A simple example of this situation is exhibited in Section 4.1.

Note that in Appendix B.2 we characterize precisely the domain of convergence of TD(0) with TN for large T and show that it changes the convergence domain of TD(0), leading to the theorem above.

On the other hand, for FR, we have

Proposition 3.2 (Convergence of Temporal Difference with Functional Regularization)**.** *If Φ, D, P^π are chosen so that TD(0) converges, then for κ small enough, for T large enough, TD(0) with Functional Regularization is guaranteed to converge.*

Proof. The proof can be found in Appendix B.3. □

The results above highlight the intuition of the last subsections: while TNs can slow down learning they also interfere with TD learning, changing its convergence domain. On the other hand, FR with appropriately chosen parameters does not impact convergence while still being able to regularize the algorithm.

Finally, note here that the results above do not mean that using TD(0) with FR is always more stable than using it with TN. When TD(0) is already unstable, depending on the interplay between the features, the off-policy distribution and the transition matrix it would be possible in some cases for TNs to make the iteration stable. However this is unlikely and show that it is impossible when the features are low dimensional (see Corollary B.4).

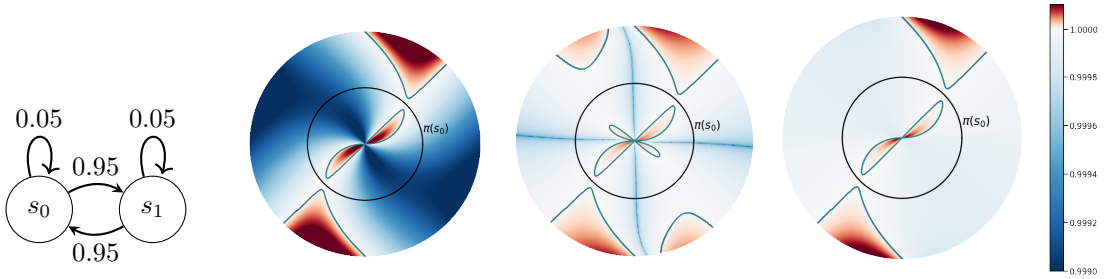

(a) **2-state MDP** (b) **TD(0)** (c) **TN** (d) **FR**

Figure 1: **2-state MDP.** We show here the spectral radius for TD(0) (b) only, (c) with Target Network, and (d) with Functional Regularization on the simple MDP (a). For any point in the disk, its radius represents the off-policy distribution of s_0 while the angle is the same as the vector $[\phi(s_0), \phi(s_1)]$. The color represents the value of the spectral radius for each method while the contour is the frontier $\rho = 1$ separating the convergence domain (shades of blue) from the divergent domain (shades of red). The black circle has a radius $\pi(s_0)$, the stationary distribution of P for which TD is guaranteed to converge as it would be on-policy.

4 Experiments

In this section, we investigate empirically the differences between FR and TN. For this, we perform three different experiments. With the first experiment, we aim at understanding the convergent and divergent behaviors of both algorithms. We use a novel visualization to give intuition and validate our theoretical results. The second experiment analyzes the stability and performance of TN and FR with respect to the regularization strength for varying degrees of off-policiness. Finally, we demonstrate that replacing TN with FR improves performance for popular algorithms on the Atari benchmark (Bellemare et al., 2013).

4.1 Simple 2-state MDP - Off Policy Evaluation

4.1.1 Experimental Set-Up

In this subsection, we visualize the behavior of TN and FR on a simple MDP. This illustrates the theory developed in Section 3 on the convergence properties of both algorithms. Baird (1995); Tsitsiklis and Van Roy (1996) and Kolter (2011) introduced simple reward-less MDPs with few states on which TD(0) can exhibit divergence. Similarly, we define a 2-state MDP in Figure 1a, which is conceptually close to Tsitsiklis and Van Roy (1996). Each state transitions to the other with probability 0.95 or transitions to itself with probability 0.05. We use 1-d features for these two states: $\phi(s_0)$ and $\phi(s_1)$. We denote the off-sampling distribution of s_0 by $d(s_0)$ and by $\pi(s_0)$ the on-policy sampling distribution of s_0 which is equal to $1/2$ in this specific case. We use $\gamma = 0.995$.

Instead of just exhibiting a single instance D, Φ for which we have divergence, we showcase the convergent or divergent behavior of TD(0), TD(0) with TN and TD(0) with FR *for all combinations* of D and Φ simultaneously. The Euclidean norm of Φ, $\|\Phi\|_2$ does not impact the convergence of any of the aforementioned algorithms as Φ can be renormalized if we scale the learning rate η by its squared norm. Therefore, only the angle of the vector $\Phi = [\phi(s_0), \phi(s_1)]$ is needed to describe all representations. In our context, there are only two states, and thus, the off-policy distribution is entirely determined by $d(s_0)$. Thus, quite naturally, one can represent the set of all representations and all off-policy distributions (D, Φ) as a disk or radius 1 [1]. In polar coordinates, the radius of a point on the disk represents $d(s_0)$ while its angle is the one of the vector Φ, i.e., $\varphi(\Phi) = \arctan \frac{\phi(s_1)}{\phi(s_0)}$.

4.1.2 Results

We draw the above-mentioned disks for the algorithms: TD(0), TD(0) with TN, and TD(0) with FR (Figure 1b, 1c, and 1d). On these disks, the colors represent the spectral radius ρ of the iteration matrix for each algorithm. Recall that $\rho < 1$ (blue) implies convergence, while $\rho > 1$ (red) implies divergence to $+\infty$. We plot the contour lines $\rho = 1$ to ease visualization. Additionally, we draw the circle of radius $d(s_0) = \pi(s_0)$ (in black), which denotes the stationary distribution. As predicted by theory, TD(0) converges on this circle for all representations. We use the regularization coefficient $\kappa = \gamma = 0.995$ and target update period $T = 10,000$ for TD(0) with TN and TD(0) with FR.

As seen in Figure 1, FR (Figure 1d) and TN (Figure 1c) show less extreme values (lighter blue) compared to TD(0) (Figure 1b). This finding implies that both the convergence and divergence are slowed down, which is expected for regularization methods.

We recover the classical divergence example for TD(0) (Tsitsiklis and Van Roy, 1996; Van Hasselt

[1] Note that we technically only need a half-disk to illustrate the convergence behavior, but we plot the whole disk for aesthetic reasons.

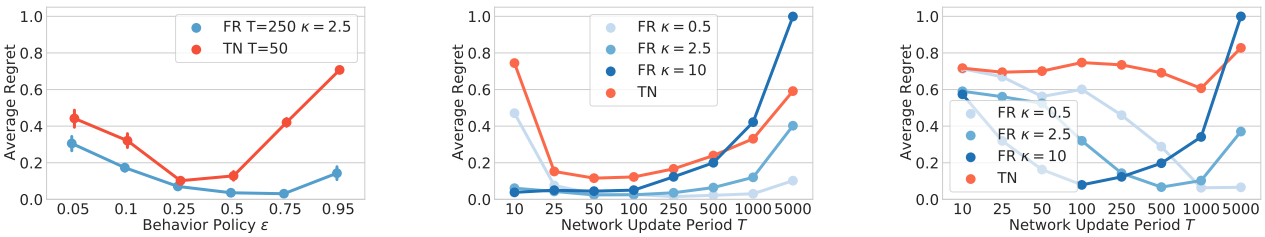

(a) **Effect of ϵ on the average regret.** (c) **Effect of T on regret for $\epsilon = 0.5$.** (e) **Effect of T on regret for $\epsilon = 0.95$.**

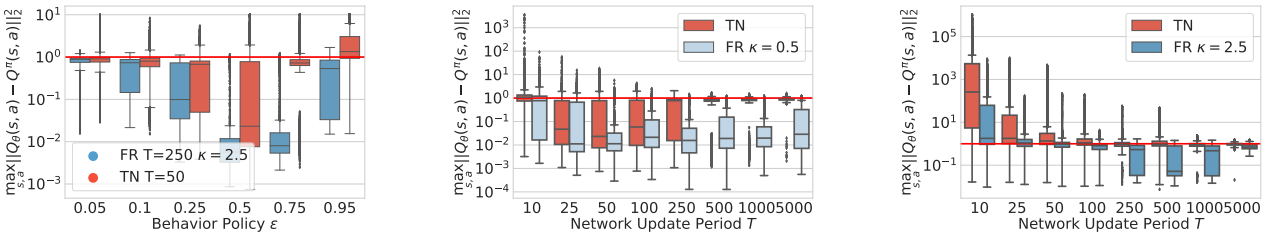

(b) **Effect of ϵ on Q-value error.** (d) **Effect of T on error for $\epsilon = 0.5$.** (f) **Effect of T on error for $\epsilon = 0.95$.**

Figure 2: **Four Rooms Comparison.** On the top row (2a, 2c and 2e) we draw the regret per episode for TN and FR for varying κ's. On the bottom row (2b, 2d and 2f) we plot the distribution of errors on the Q-value for the same set of algorithms. Each of the three columns represents one experimental setting. In the first column, we vary the degree of "off-policiness" (via ϵ) and report the best-performing algorithms. In the last two columns, we fix ϵ and show the impact of the target update period T and the behavior policy exploration noise ϵ on performance and Q-error.

et al., 2018): if $\phi(s_1) > \phi(s_0) > 0$ and the behavior distribution $d(s_0)$ is close to 1, the point $(d(s_0), \varphi(\Phi))$ in polar coordinates lies in the large upper red region of Figure 1b, thus TD(0) will diverge.

As proved in Proposition 3.2, the convergence domain of TD(0) with FR is similar to the one of TD(0). Interestingly, and as shown in Theorem 3.1, TD(0) with TN may diverge in regions where TD(0) with FR does not. For example, in Figure 1c we see four smaller (symmetric) additional divergence regions (red) in the lower right and upper left regions of the disk for $d(s_0)$ close to 1 and two symmetric ones near the center of the disk. This can happen when $\Phi^\top D P^\pi \Phi$ which appears in the implicit regularization of TN has negative eigenvalues.

These depictions of the convergence or divergence behaviors of TD(0) with FR and TD(0) with TN hint at the fact that TN-based algorithms may be more unstable than FR-based algorithms for strongly off-policy distributions. This hypothesis is studied empirically in the next subsection. We provide more figures in Appendix C.1 where we also discuss the impact of the discount factor γ.

4.2 Four Rooms

4.2.1 Experimental Set-Up

In this section, we investigate the impact of changing the regularization strength and the off-policy distribution for both TN and FR. These experiments are run in the Four Rooms environment (Sutton et al., 1999) (Figure 6 in Appendix) which is comprised of four rooms divided by walls with a single gap in each wall allowing an agent to move between rooms. The environment size is 11×11. The agent's position is given by a one-hot encoding. The agent's available actions are up, down, left, and right. The agent starts in the bottom right position and must reach the goal in the top left position. The rationale for using this environment is that it allows us to compute the true Q values, which can then be compared with the ones learned by our Q-function approximator, a DNN composed of 2 hidden layers (details in Table 2).

To study the behavior of TN and FR under different off-policy data collections, the data is collected under a behavior policy that takes a random action with probability ϵ and takes $\mathbf{a} = \arg\max_{\mathbf{a}} Q_w(\mathbf{s}, \mathbf{a})$ with probability $1 - \epsilon$. As ϵ tends towards 1, the data collection becomes more off-policy and makes the Q-value estimation more difficult.

During training we measure $\max_{\mathbf{s},\mathbf{a}} \|Q_w(\mathbf{s}, \mathbf{a}) - Q^\pi(\mathbf{s}, \mathbf{a})\|_2^2$, where Q^π was obtained in closed form

and π is the greedy policy. In Figure 2b, 2d, 2f, the red line indicates an error of 1, and in our MDP, all true Q-values are between 0 and 1. Thus any point above the red line has Q-value estimates outside of this feasible range, indicating soft-divergence (Van Hasselt et al., 2018). We also evaluate the average per-episode regret for 100 episodes collected under $\epsilon_{\text{eval}}-$greedy policy with $\epsilon_{\text{eval}} = 0.1$ as it is common for RL agents in deterministic environments such as the Atari suite.

4.2.2 Results

Figures 2a and 2b: Best hyper-parameters over all ϵ. For both methods, we observe a large average regret for smaller ϵ which is due to less exploration early on. On the other hand, the average regret is increased for larger ϵ due to the behavior policy being more off-policy. Furthermore, we observe that for near-on-policy data collection, the difference in performance between TN and FR is negligible. However, for a behavior policy with $\epsilon \geq 0.5$, the difference in performance increases, and TN performs much worse than FR. While FR, by itself, does not impact exploration, its increased stability allows us to learn from more exploratory policies than TN (larger ϵ). To better understand the additional flexibility provided by κ, we closely investigate the behavior policy $\epsilon = 0.5$ and $\epsilon = 0.95$.

Figures 2c and 2d: Behavior Policy with $\epsilon = 0.5$. In Figure 2c, we observe that TN's performance improves as we increase T until it reaches 100, then the performance degrades. Interestingly, the poor performances for small and large T are caused by two different reasons. On the one hand, for $T = 10$, we observe a median error slightly above 1 indicating soft-divergence which results in high regret Figure 2c. As we increase T up to 250, we can see that the median error decreases and that the outliers are also less extreme. This translates into better average regrets. On the other hand, as we increase T past 250 the distribution of errors is concentrated slightly below 1, and the average regret is high again. This can be understood as TN over-regularizing which greatly slows down training.

The behavior is quite different for FR with $\kappa = 0.5$. For $T = 10$, the median error is close to 1 and there are a few outliers that result in a high average regret. As T increases the median error falls until T reaches 250 where the lowest average regret is achieved. As T increases past 250, the error and the regret slightly increase hinting that the regularization might be too strong.

Figures 2e and 2f: Behavior Policy with $\epsilon = 0.95$. In Figure 2e for FR $\kappa = 2.5$, we observe that the regret decreases as we increase T up to 500. This indicates that increasing regularization is beneficial as can be seen by the reduction in median error in Figure 2f. For T larger than 500, the regret and the median error increase indicating over-regularization, thus slowing down learning. For $T = 10$, TN and FR $\kappa = 2.5$ have similar regret and error, but as we increase T, TN's regret does not improve. This can be explained by carefully examining Figure 2f. We can see that the error stays very close to 1 which indicates over-regularization, leading to as slow training.

In summary, we have shown that changing the update period T combined with Target Networks is not a regularizer flexible enough to obtain good performance. On the other hand, FR can reach higher performance by tuning κ and T jointly as it results in better regularization trade-offs.

4.3 Atari

4.3.1 Experimental Set-Up

The Arcade Learning Environment (Bellemare et al., 2013) provides a set of benchmark Atari games for evaluating RL agents. These environments are a popular benchmark as they possess rich visual observations and diverse reward functions. We evaluate the impact of using Functional Regularization instead of Target Networks on several RL algorithms.

As we observed in Section 4.2.2, tuning T and κ can result in great performance gains and we encourage practitioners to perform a sweep over these two hyper-parameters if possible. However, due to the computational constraints of the Atari benchmark, we only tuned κ and used the same T as the one used by TN. All results are reported in Table 1.

We used the baselines provided in the DQN Zoo library (Quan and Ostrovski, 2020) and easily replaced the Target Network loss with Functional Regularization loss in a few lines of code using Jax (Bradbury et al., 2018) and Haiku (Hennigan et al., 2020). For DQN and Double DQN, we tuned κ for each FR agent by performing experiments on 2 seeds (only 1 set of global hyper-parameters was used for every task). Once the best set of hyper-parameters for each method has been selected, we used 10 additional seeds (and exclude the 2 initial seeds) to compare the algorithms. All hyper-parameters we used are displayed in Table 3 in the Appendix. We used the same suite of representative environments used in Mnih et al. (2013)[2]. Each seed took 48 hours to run on our resources for a total of 14,400 hours of GPU usage. Additional experimental details can be found in the Appendix.

4.3.2 Results

Comparison with DQN. DQN (Mnih et al., 2013) was the first RL algorithm to reach human performance on a subset of the Atari suite. It learns the value function by minimizing the TN loss as defined in Equation (4). We re-

[2]excluding Pong for which all algorithms achieve the same high performance.

Table 1: **Atari Comparisons.** We report the average of the last 10 test episodes on the Atari benchmark and the standard error. See Appendix A, Figures 7, 8, and 9 for full training curves.

Environment Agent	Beam Rider	Breakout	Enduro	Qbert	Seaquest	Space Invaders
TN DQN	7266 +/- 112	320 +/- 6	463 +/- 22	7321 +/- 412	2392 +/- 246	1375 +/- 46
FR DQN $\kappa = 0.75$ (Ours)	**7939 +/- 138**	**339 +/- 4**	**576 +/- 22**	**10118 +/- 346**	**3387 +/- 334**	**1495 +/- 38**
TN Double DQN	**12316 +/- 259**	310 +/- 7	693 +/- 44	11890 +/- 277	**10638 +/- 454**	2009 +/- 46
FR Double DQN $\kappa = 0.75$ (Ours)	11739 +/- 285	**383 +/- 3**	**1181 +/- 28**	**12705 +/- 211**	7124 +/- 2160	**2692 +/- 120**
TN Rainbow	15398 +/- 816	**375 +/- 1**	2307 +/- 7	30911 +/- 666	18916 +/- 7130	9907 +/- 3055
FR Rainbow $\kappa = 2.5$ (Ours)	**18216 +/- 757**	350 +/- 5	2302 +/- 8	31521 +/- 1115	22976 +/- 12546	**17127 +/- 3117**

place the TN loss by the FR loss defined in Equation (7). Across all environments, using the FR loss with a $\kappa = 0.75$ significantly improves the performance of the DQN algorithm. Additionally, Figure 7 in Appendix C.3 presents the training curves for FR DQN, TN DQN, and other baselines such as Polyak DQN.

Comparison with Double DQN. Similarly to DQN, Double DQN (Van Hasselt, 2010) minimizes the TN loss, but decouples the "action-selection" from the "action-evaluation" to estimate the next value function countering the maximum bias. Double DQN has been shown to significantly improves upon DQN on the Atari suite. We observe that replacing the TN loss with the FR loss significantly improves the performance of Double DQN on 4 of the 6 Atari games studied. The training curves are provided in Figure 8.

Comparison with Rainbow DQN. Rainbow DQN (Hessel et al., 2018) obtains state-of-the-art results on the Atari benchmark. Rainbow learn the values by using a very sophisticated objective. Specifically, they use multi-step returns as a way to trade-off between bias and variance of the target value. Additionally, they use distributional DQN (Bellemare et al., 2017) which requires to discretize the Q value, to project the target between -10 and 10, and to minimize the Wasserstein metric. Furthermore, they use noisy network to improve exploration (Fortunato et al., 2017), prioritized experience replay (Schaul et al., 2015), and dueling networks. Overall, Rainbow requires 12 additional hyper-parameters. For simplicity, we kept all the hyper-parameters constant and simply tuned κ when introducing Functional Regularization. We observe that replacing TN with FR matches Rainbow on 3 tasks, outperforms it on 2 tasks, and under-performs it on Breakout. See Figure 9 for the training curves.

In summary, we have shown that the FR loss can be used as a drop-in replacement for the TN loss across a variety of RL algorithms - even by keeping all hyper-parameters fixed. We observed that using the FR loss instead of the TN loss drastically improves the performances of DQN and Double DQN, but that its effectiveness decreases as it is combined with more sophisticated methods, i.e. Rainbow DQN.

5 Related work

Multiple previous works have investigated how to improve value estimation through various constraints and regularizations. Shao et al. (2020) proposed adding an additional backward Squared Bellman Error loss to the next Q-value to stabilize training and remove the need for a target network on some control problems. Farahmand et al. (2009) is perhaps the closest work to our own, they regularize the L_2 norm of the Q-value estimates, i.e., penalizing $\kappa||Q_w||^2$. However, penalizing the magnitude of the Q-values would prevent the algorithm from converging to Q^* if κ does not tend towards 0. Penalizing the output of a DNN draws connections with popular regularization methods in the field of policy optimization which were inspired by trust-region algorithms (Schulman et al., 2015a; Abdolmaleki et al., 2018b,a) in which the policy is KL regularized towards its past values. In the same spirit, for value-based methods, our proposed Functional Regularization regularizes the Q function estimates towards their past values. Alternatively, Kim et al. (2019) showed that by using the mellow max operator as an alternative to the max operator used in bootstrapping, it was possible to stabilize training and train without a target network on some Atari games.

Other works have sought to stabilize the Q-value estimates by constraining parameter updates, e.g., through regularization (Farebrother et al., 2018), conjugate gradient methods (Schulman et al., 2015b), pre-conditioning the gradient updates (Knight and Lerner, 2018; Achiam et al., 2019), or using Kalman filtering (Shashua and Mannor, 2019, 2020). However, weight regularization might be ineffective in DNNs. For neural networks, the network outputs depend on the weights in a complex way and the exact value of the weights may not matter much. What ultimately matters is the network outputs (Benjamin et al., 2018; Khan et al., 2019), and it is better to directly regularize those. For instance, while Polyak's averaging (Lillicrap et al., 2015), a common weight regularization technique, has found success in control problems (Haarnoja et al., 2018; Fujimoto

et al., 2018), periodically updating the parameters is usually preferred for complex DNN architectures (Mnih et al., 2013; Hausknecht and Stone, 2015; Hessel et al., 2018; Kapturowski et al., 2018; Parisotto et al., 2020).

Finally, neither FR nor TN have convergence guarantees for all representations and off-policy distributions when using bootstrapping: they still suffer from the deadly triad (Sutton, 1995; Tsitsiklis and Van Roy, 1997; Sutton and Barto, 2018) as shown in Section 3. Several works have proposed algorithms with stronger convergence guarantees such as gradient TD methods (Sutton et al., 2008, 2009), TDC (Maei et al., 2009) or Emphatic weights (Sutton et al., 2016). However, these methods are often computationally significantly more expensive or haven't been shown to scale favorably with DNNs. Recently (Zhang et al., 2021) studied how Target Networks can help stabilize the TD algorithm, which is seemingly at odds with our Theorem 3.1. However, in their paper, they study a variant of DQN with TN which involves projection steps while our analysis focuses on the version used in practice.

6 Conclusion

In this paper, we cast a light on the implicit regularization performed by using Target Networks in RL. We have shown that despite being used as a regularizer Target Networks can cause instabilities while also being inflexible as the regularization depends on the discount factor γ. To overcome these issues, we introduced Functional Regularization which directly regularizes the value network towards a network parameterized by lagging parameters.

We demonstrated empirically in a 2-state MDP that using Target Networks is a poor regularizer and can unstabilize TD for off-policy data. In opposition, Functional Regularization does not suffer from these issues and effectively slows down the optimization.

Furthermore, in the Four Rooms domain, we show that changing the update period T is not enough to have a flexible regularizer for Target Networks. On the other hand, for Functional Regularization, by controlling the regularization scaling parameter κ, we can obtain better regularization trade-offs than by varying T only. This is further exacerbated when the "off-policiness" is high.

Finally, we have shown that Functional Regularization can be used as a drop-in replacement for Target Networks on 3 popular RL algorithms resulting in matching or outperforming Target Networks for most of the scenarios studied.

References

Abdolmaleki, A., Springenberg, J. T., Degrave, J., Bohez, S., Tassa, Y., Belov, D., Heess, N., and Riedmiller, M. (2018a). Relative entropy regularized policy iteration. *arXiv preprint arXiv:1812.02256*.

Abdolmaleki, A., Springenberg, J. T., Tassa, Y., Munos, R., Heess, N., and Riedmiller, M. (2018b). Maximum a posteriori policy optimisation. *arXiv preprint arXiv:1806.06920*.

Achiam, J., Knight, E., and Abbeel, P. (2019). Towards characterizing divergence in deep q-learning. *arXiv preprint arXiv:1903.08894*.

Baird, L. (1995). Residual algorithms: Reinforcement learning with function approximation. In *Machine Learning Proceedings 1995*, pages 30–37. Elsevier.

Bellemare, M. G., Dabney, W., and Munos, R. (2017). A distributional perspective on reinforcement learning. In *International Conference on Machine Learning*, pages 449–458. PMLR.

Bellemare, M. G., Naddaf, Y., Veness, J., and Bowling, M. (2013). The arcade learning environment: An evaluation platform for general agents. *Journal of Artificial Intelligence Research*, 47:253–279.

Bellman, R. (1966). Dynamic programming. *Science*, 153(3731):34–37.

Benjamin, A. S., Rolnick, D., and Kording, K. (2018). Measuring and regularizing networks in function space. *arXiv preprint arXiv:1805.08289*.

Bertsekas, D. P. and Tsitsiklis, J. N. (1996). *Neuro-dynamic programming*. Athena Scientific.

Bradbury, J., Frostig, R., Hawkins, P., Johnson, M. J., Leary, C., Maclaurin, D., Necula, G., Paszke, A., VanderPlas, J., Wanderman-Milne, S., and Zhang, Q. (2018). JAX: composable transformations of Python+NumPy programs.

Farahmand, A. M., Ghavamzadeh, M., Szepesvári, C., and Mannor, S. (2009). Regularized fitted q-iteration for planning in continuous-space markovian decision problems. In *2009 American Control Conference*, pages 725–730. IEEE.

Farebrother, J., Machado, M. C., and Bowling, M. (2018). Generalization and regularization in dqn. *arXiv preprint arXiv:1810.00123*.

Fortunato, M., Azar, M. G., Piot, B., Menick, J., Osband, I., Graves, A., Mnih, V., Munos, R., Hassabis, D., Pietquin, O., et al. (2017). Noisy networks for exploration. *arXiv preprint arXiv:1706.10295*.

Fujimoto, S., Hoof, H., and Meger, D. (2018). Addressing function approximation error in actor-critic methods. In *International Conference on Machine Learning*, pages 1587–1596. PMLR.

Haarnoja, T., Zhou, A., Abbeel, P., and Levine, S. (2018). Soft actor-critic: Off-policy maximum entropy deep reinforcement learning with a stochastic actor. In *International Conference on Machine Learning*, pages 1861–1870. PMLR.

Hausknecht, M. and Stone, P. (2015). Deep recurrent q-learning for partially observable mdps. *arXiv preprint arXiv:1507.06527*.

Hennigan, T., Cai, T., Norman, T., and Babuschkin, I. (2020). Haiku: Sonnet for JAX.

Hessel, M., Modayil, J., Van Hasselt, H., Schaul, T., Ostrovski, G., Dabney, W., Horgan, D., Piot, B., Azar, M., and Silver, D. (2018). Rainbow: Combining improvements in deep reinforcement learning. In *Proceedings of the AAAI Conference on Artificial Intelligence*, volume 32.

Kapturowski, S., Ostrovski, G., Quan, J., Munos, R., and Dabney, W. (2018). Recurrent experience replay in distributed reinforcement learning. In *International conference on learning representations*.

Khan, M. E. E., Immer, A., Abedi, E., and Korzepa, M. (2019). Approximate inference turns deep networks into gaussian processes. In *Advances in neural information processing systems*, pages 3094–3104.

Kim, S., Asadi, K., Littman, M., and Konidaris, G. (2019). Deepmellow: removing the need for a target network in deep q-learning. In *Proceedings of the Twenty Eighth International Joint Conference on Artificial Intelligence*.

Kingma, D. P. and Ba, J. (2014). Adam: A method for stochastic optimization. *arXiv preprint arXiv:1412.6980*.

Knight, E. and Lerner, O. (2018). Natural gradient deep q-learning. *arXiv preprint arXiv:1803.07482*.

Kolter, J. (2011). The fixed points of off-policy td. *Advances in Neural Information Processing Systems*, 24:2169–2177.

Lillicrap, T. P., Hunt, J. J., Pritzel, A., Heess, N., Erez, T., Tassa, Y., Silver, D., and Wierstra, D. (2015). Continuous control with deep reinforcement learning. *arXiv preprint arXiv:1509.02971*.

Lyapunov, A. M. (1992). The general problem of the stability of motion. *International journal of control*, 55(3):531–534.

Maei, H. R., Szepesvari, C., Bhatnagar, S., Precup, D., Silver, D., and Sutton, R. S. (2009). Convergent temporal-difference learning with arbitrary smooth function approximation. In *NIPS*, pages 1204–1212.

Mnih, V., Kavukcuoglu, K., Silver, D., Graves, A., Antonoglou, I., Wierstra, D., and Riedmiller, M. (2013). Playing atari with deep reinforcement learning. *arXiv preprint arXiv:1312.5602*.

Parisotto, E., Song, F., Rae, J., Pascanu, R., Gulcehre, C., Jayakumar, S., Jaderberg, M., Kaufman, R. L., Clark, A., Noury, S., et al. (2020). Stabilizing transformers for reinforcement learning. In *International Conference on Machine Learning*, pages 7487–7498. PMLR.

Puterman, M. L. (2014). *Markov decision processes: discrete stochastic dynamic programming*. John Wiley & Sons.

Quan, J. and Ostrovski, G. (2020). DQN Zoo: Reference implementations of DQN-based agents.

Schaul, T., Quan, J., Antonoglou, I., and Silver, D. (2015). Prioritized experience replay. *arXiv preprint arXiv:1511.05952*.

Schulman, J., Levine, S., Abbeel, P., Jordan, M., and Moritz, P. (2015a). Trust region policy optimization. In *International conference on machine learning*, pages 1889–1897. PMLR.

Schulman, J., Moritz, P., Levine, S., Jordan, M., and Abbeel, P. (2015b). High-dimensional continuous control using generalized advantage estimation. *arXiv preprint arXiv:1506.02438*.

Shao, L., You, Y., Yan, M., Sun, Q., and Bohg, J. (2020). Grac: Self-guided and self-regularized actor-critic. *arXiv preprint arXiv:2009.08973*.

Shashua, S. D.-C. and Mannor, S. (2019). Trust region value optimization using kalman filtering. *arXiv preprint arXiv:1901.07860*.

Shashua, S. D.-C. and Mannor, S. (2020). Kalman meets bellman: Improving policy evaluation through value tracking. *arXiv preprint arXiv:2002.07171*.

Sutton, R. S. (1988). Learning to predict by the methods of temporal differences. *Machine learning*, 3(1):9–44.

Sutton, R. S. (1995). On the virtues of linear learning and trajectory distributions. In *Proceedings of the Workshop on Value Function Approximation, Machine Learning Conference*, page 85.

Sutton, R. S. and Barto, A. G. (2018). *Reinforcement learning: An introduction*. MIT press.

Sutton, R. S., Maei, H. R., Precup, D., Bhatnagar, S., Silver, D., Szepesvári, C., and Wiewiora, E. (2009). Fast gradient-descent methods for temporal-difference learning with linear function approximation. In *Proceedings of the 26th Annual International Conference on Machine Learning*, pages 993–1000.

Sutton, R. S., Mahmood, A. R., and White, M. (2016). An emphatic approach to the problem of off-policy temporal-difference learning. *The Journal of Machine Learning Research*, 17(1):2603–2631.

Sutton, R. S., Precup, D., and Singh, S. (1999). Between mdps and semi-mdps: A framework for temporal abstraction in reinforcement learning. *Artificial intelligence*, 112(1-2):181–211.

Sutton, R. S., Szepesvári, C., and Maei, H. R. (2008). A convergent o (n) algorithm for off-policy temporal-difference learning with linear function approximation. *Advances in neural information processing systems*, 21(21):1609–1616.

Tihonov, A. N. (1963). Solution of incorrectly formulated problems and the regularization method. *Soviet Math.*, 4:1035–1038.

Tikhonov, A. N. (1943). On the stability of inverse problems. In *Dokl. Akad. Nauk SSSR*, volume 39, pages 195–198.

Tsitsiklis, J. N. and Van Roy, B. (1996). Feature-based methods for large scale dynamic programming. *Machine Learning*, 22(1):59–94.

Tsitsiklis, J. N. and Van Roy, B. (1997). Analysis of temporal-diffference learning with function approximation. In *Advances in neural information processing systems*, pages 1075–1081.

Van Hasselt, H. (2010). Double q-learning. *Advances in neural information processing systems*, 23:2613–2621.

Van Hasselt, H., Doron, Y., Strub, F., Hessel, M., Sonnerat, N., and Modayil, J. (2018). Deep reinforcement learning and the deadly triad. *arXiv preprint arXiv:1812.02648*.

Van Hasselt, H., Guez, A., and Silver, D. (2016). Deep reinforcement learning with double q-learning. In *Proceedings of the AAAI Conference on Artificial Intelligence*, volume 30.

Zhang, S., Yao, H., and Whiteson, S. (2021). Breaking the deadly triad with a target network. In *International Conference on Machine Learning*, pages 12621–12631. PMLR.

A Appendix

A.1 Q-learning with Target Network

Letting $R^{(t)} \equiv R(\mathbf{s}_t, \mathbf{a}_t)$, $Q^{(t)} \equiv Q(\mathbf{s}_t, \mathbf{a}_t)$ and $\Delta Q_{\bar{w}}^{(t)} \equiv \mathbb{E}[Q_{\bar{w}}^{(t+1)} - Q_{\bar{w}}^{(t)} | \mathbf{s}_t, \mathbf{a}_t] = \mathbb{E}[Q_{\bar{w}}^{(t+1)} | \mathbf{s}_t, \mathbf{a}_t] - Q_{\bar{w}}^{(t)}$

$$
\begin{aligned}
\nabla_w l^{\text{target}}(w) &= -\big(R^{(t)} + \gamma \mathbb{E}_{P,\pi}[Q_{\bar{w}}^{(t+1)}] - Q_w^{(t)}\big) \nabla_w Q_w^{(t)} \\
&= -\big(R^{(t)} + \gamma (Q_{\bar{w}}^{(t)} + \Delta Q_{\bar{w}}^{(t)}) - Q_w^{(t)}\big) \nabla_w Q_w^{(t)} \\
&= -\big(R^{(t)} + \gamma (Q_{\bar{w}}^{(t)} + \Delta Q_{\bar{w}}^{(t)}) - (1 - \gamma + \gamma) Q_w^{(t)}\big) \nabla_w Q_w^{(t)} \\
&= -\big(R^{(t)} + \gamma Q_{\bar{w}}^{(t)} + \gamma \Delta Q_{\bar{w}}^{(t)} - (1 - \gamma) Q_w^{(t)} - \gamma Q_w^{(t)}\big) \nabla_w Q_w^{(t)} \\
&= -\big(R^{(t)} + \gamma \Delta Q_{\bar{w}}^{(t)} - (1 - \gamma) Q_w^{(t)}\big) \nabla_w Q_w^{(t)} + \gamma \big(Q_{\bar{w}}^{(t)} - Q_w^{t}\big) \nabla_w Q_w^{(t)} \\
&= -\big(R^{(t)} + \gamma \Delta Q_{\bar{w}}^{(t)} - Q_w^{(t)} + \gamma Q_w^{(t)}\big) \nabla_w Q_w^{(t)} + \gamma \big(Q_{\bar{w}}^{(t)} - Q_w^{(t)}\big) \nabla_w Q_w^{(t)} \\
&= -\big(R^{(t)} + \gamma (Q_w^{(t)} + \underline{\Delta Q_{\bar{w}}^{(t)}}) - Q_w^{(t)}\big) \nabla_w Q_w^{(t)} + \underline{\gamma} \big(Q_{\bar{w}}^{(t)} - Q_w^{(t)}\big) \nabla_w Q_w^{(t)}
\end{aligned}
$$

A.2 Q-learning with Functional Regularization

$$
\begin{aligned}
\nabla_w l^{\text{FR}}(w) &= -\big(R^{(t)} + \gamma \mathbb{E}_{P,\pi}[Q_w^{(t+1)}] - Q_w^{(t)}\big) \nabla_w Q_w^{(t)} + \kappa \big(Q_{\bar{w}}^{t} - Q_w^{(t)}\big) \nabla Q_w^{(t)} \\
&= -\big(R^{(t)} + \gamma (Q_\theta^{(t)} + \underline{\Delta Q_\theta^{(t)}}) - Q_w^{(t)}\big) \nabla_w Q_w^{(t)} + \underline{\kappa} \big(Q_{\bar{w}}^{(t)} - Q_w^{t}\big) \nabla Q_w^{(t)}
\end{aligned}
$$

A.3 Polyak Averaging

To better understand the implicit regularization perform by Polyak averaging, let us consider a situation in which after each gradient step (indexed by i), we identified the target network as the solution to the problem:

$$
\bar{w}_{i+1} = \min_{\bar{w}} \frac{1}{2} \|\bar{w} - w\|^2 + \frac{1 - \tau}{2\tau} \|\bar{w} - \bar{w}_i\|^2 \tag{8}
$$

whereby w is the latest set of weights of the Q-network and $\bar{w}_i$ is the previous instance of the target network, and τ is the exponential averaging step size. Minimizing $\bar{w}$ is obtained by computing the gradient of the problem and equating it 0, leading to $\bar{w}_{i+1} = (1 - \tau) w + \tau \bar{w}$, which is exactly Polyak's updating. This derivation illustrates that Polyak's update is indeed a form of weight regularization with respect to the most recent target network weights.

B Proofs for Linear Function Approximation case

B.1 Supporting lemma

Lemma B.1 (Difference of inverses)**.** *For A and B two non-singular matrices*

$$
A^{-1} - B^{-1} = A^{-1}(B - A)B^{-1}
$$

Proof. We multiply each side by A on the left and B on the right and show they are equal. Left hand term:

$$
A(A^{-1} - B^{-1})B = B - A
$$

And for the right hand term:

$$
AA^{-1}(B - A)B^{-1}B = B - A
$$

By equating both terms and multiplying by A^{-1} on the left and B^{-1} on the right we have the equality.

□

Proposition B.2 (Convergence of TD-TN)**.** *For $\Pi_\Phi = \Phi(\Phi^\top D \Phi)^{-1} \Phi^\top D$, the projection matrix onto the span of Φ, if $\rho(\Pi_\Phi P^\pi) < \frac{1}{\gamma}$ then for T large enough, Target Network Value Iteration is guaranteed to converge.*

B.2 Proof for the domain of convergence of TD(0) with TN

The solution for the TD iteration is

$$\boxed{w^* = (\Phi D(I - \gamma P^\pi)\Phi)^{-1}\Phi^\top DR} \tag{9}$$

B.2.1 Regularized iteration

Let us call $\bar{w}$ the frozen weight. We consider in this subsection only the "inner loop iteration", i.e the ones for a fixed frozen weight vector. The update for TD with target network is

$$w_{t+1} = w_t + \eta\Phi^\top D(R + \gamma P^\pi \Phi\bar{w} - \Phi w_t)$$

We call $w^*(\bar{w})$ the fixed point of that iteration rule which satisfies

$$\boxed{w^*(\bar{w}) = (\Phi^\top D\Phi)^{-1}\Phi^\top D(R + \gamma P^\pi \Phi\bar{w})} \tag{10}$$

Thus our updates satisfy

$$\begin{aligned}
w_{t+1} - w^*(\bar{w}) &= w_t + \eta\Phi^\top D(R + \gamma P^\pi \Phi\bar{w} - \Phi w_t) - w^*(\bar{w}) \\
&= (I - \eta\Phi^\top D\Phi)w_t + \eta\Phi^\top D(R + \gamma P^\pi \Phi\bar{w}) - w^*(\bar{w}) \\
&= (I - \eta\Phi^\top D\Phi)w_t + \eta\Phi^\top D\Phi w^*(\bar{w}) - w^*(\bar{w}), \text{using 10} \\
&= (I - \eta\Phi^\top D\Phi)(w_t - w^*(\bar{w}))
\end{aligned}$$

So

$$\boxed{w_t - w^*(\bar{w}) = (I - \eta\Phi^\top D\Phi)^t(w_0 - w^*(\bar{w}))} \tag{11}$$

As $\Phi^\top D\Phi$ is symmetric real with positive eigenvalues, $\eta \leq \frac{2}{\lambda_1}$ with λ_1 its largest eigenvalue, w_t is guaranteed to converge linearly to $w^*(\bar{w})$.

B.2.2 Distance between regularized and original optima

Now we look at the vector $w^*(\bar{w}) - w^*$

$$\begin{aligned}
w^*(\bar{w}) - w^* &= (\Phi^\top D\Phi)^{-1}\Phi^\top D(R + \gamma P^\pi \Phi\bar{w}) - (\Phi D(I - \gamma P^\pi)\Phi)^{-1}\Phi DR \\
&= ((\Phi^\top D\Phi)^{-1} - (\Phi^\top D(I - \gamma P^\pi)\Phi)^{-1})\Phi^\top DR + (\Phi^\top D\Phi)^{-1}\gamma\Phi^\top DP^\pi\Phi\bar{w} \\
&= -\gamma(\Phi^\top D\Phi)^{-1}\Phi^\top DP^\pi\Phi(\Phi D(I - \gamma P^\pi)\Phi)^{-1})\Phi^\top DR + \gamma(\Phi^\top D\Phi)^{-1}\Phi^\top DP\Phi\bar{w}, \text{ using Lemma B.1} \\
&= -\gamma(\Phi^\top D\Phi)^{-1}\Phi^\top DP^\pi\Phi w^* + \gamma(\Phi^\top D\Phi)^{-1}\Phi^\top DP\Phi\bar{w}, \text{ By definition of } w^* \\
&= \gamma(\Phi^\top D\Phi)^{-1}\Phi^\top DP^\pi\Phi(\bar{w} - w^*)
\end{aligned}$$

We summarize it here, this is the bias between the regularized and true optima

$$\boxed{w^*(\bar{w}) - w^* = \gamma(\Phi^\top D\Phi)^{-1}\Phi^\top DP^\pi\Phi(\bar{w} - w^*)} \tag{12}$$

B.2.3 Distance between inner loop iterate and optimum

$$\begin{aligned}
\mathcal{T}_K(\bar{w}) - w^* &= \mathcal{T}_K(\bar{w}) - w^*(\bar{w}) + w^*(\bar{w}) - w^* \\
&= (I - \eta\Phi^\top D\Phi)^K(\bar{w} - w^*(\bar{w}) + \gamma(\Phi^\top D\Phi)^{-1}\Phi^\top DP^\pi\Phi(\bar{w} - w^*) \\
&= (I - \eta\Phi^\top D\Phi)^K(\bar{w} - w^* - (w^*(\bar{w}) - w^*)) + \gamma(\Phi^\top D\Phi)^{-1}\Phi^\top DP^\pi\Phi(\bar{w} - w^*) \\
&= [(I - \eta\Phi^\top D\Phi)^K(I - \gamma(\Phi^\top D\Phi)^{-1}\Phi^\top DP^\pi\Phi) + \gamma(\Phi^\top D\Phi)^{-1}\Phi^\top DP^\pi\Phi](\bar{w} - w^*)
\end{aligned}$$

It is possible to rewrite it in value space by multiplying by Φ on the left

$$\begin{aligned}
\mathcal{T}_K(\bar{Q}) - Q^* &= \Phi(I - \eta\Phi^\top D\Phi)^K(I - \gamma(\Phi^\top D\Phi)^{-1}\Phi^\top DP^\pi)(\bar{Q} - Q^*) + \gamma\Phi(\Phi^\top D\Phi)^{-1}\Phi^\top DP^\pi\Phi(\bar{w} - w^*) \\
&= \Phi(I - \eta\Phi^\top D\Phi)^{K-1}((\Phi^\top D\Phi)^{-1} - \eta I)\Phi^\top D\Phi(I - \gamma(\Phi^\top D\Phi)^{-1}\Phi^\top DP^\pi\Phi)(\bar{w} - w^*) + \gamma\Pi_\Phi P^\pi(\bar{Q} - Q^*) \\
&= \Phi(I - \eta\Phi^\top D\Phi)^{K-1}((\Phi^\top D\Phi)^{-1} - \eta I)\Phi^\top D(I - \gamma\Phi(\Phi^\top D\Phi)^{-1}\Phi^\top DP^\pi\Phi)(\bar{Q} - Q^*) + \gamma\Pi_\Phi P^\pi(\bar{Q} - Q^*) \\
&= \Phi(I - \eta\Phi^\top D\Phi)^{K-1}((\Phi^\top D\Phi)^{-1} - \eta I)\Phi^\top D(I - \gamma\Pi_\Phi P^\pi)(\bar{Q} - Q^*) + \gamma\Pi_\Phi P^\pi(\bar{Q} - Q^*) \\
&= \big[\Phi(I - \eta\Phi^\top D\Phi)^{K-1}((\Phi^\top D\Phi)^{-1} - \eta I)\Phi^\top D(I - \gamma\Pi_\Phi P^\pi) + \gamma\Pi_\Phi P^\pi\big](\bar{Q} - Q^*)
\end{aligned}$$

The interesting bit here when analyzing how this behaves for large K is that $(I - \eta\Phi^\top D\Phi)^{K-1}$ is essentially a matrix that can become arbitrarily small when K is large.

$$\mathcal{T}_\infty(Q(\bar{w})) - Q^* = \gamma\Pi_\Phi P^\pi(Q(\bar{w}) - Q^*) \tag{13}$$

This is guaranteed to converge if $\Pi_\Phi P$ is a contraction, which is the case for instance when D is the stationary distribution of P.

Also as $Q^* = \Phi w^*$ is the fixed point of the projected Bellman iteration, we have

$$\mathcal{T}_\infty(Q(\bar{w})) = \Pi_\Phi\big(R + \gamma P^\pi Q(\bar{w})\big)$$

This is the *projected value iteration* or *projected policy evaluation* algorithm (Bertsekas and Tsitsiklis, 1996).

B.2.4 Continuity of norms and spectral radius

Now if we suppose that $\rho(\Pi_\Phi P^\pi) < \frac{1}{\gamma}$ or written differently $\rho(\gamma\Pi_\Phi P^\pi) \leq \alpha < 1$, as ρ is a continuous function of its input entries, for K large enough, we can guarantee that

$$\forall\epsilon > 0, \exists K \in \mathbb{N} / \rho(\Phi(I - \eta\Phi^\top D\Phi)^{K-1}((\Phi^\top D\Phi)^{-1} - \eta I)\Phi^\top D(I - \gamma\Pi_\Phi P^\pi\Phi) + \gamma\Pi_\Phi P^\pi) < \alpha + \epsilon$$

In particular for $\epsilon < 1 - \alpha$ which would ensure the convergence of the algorithm.

The lower bound on K can be made more precise using the Bauer-Fike theorem $\rho(A + B) \leq \rho(A) + \|B\|\kappa(P_A)$

We can write

$$\begin{aligned}
\rho_K &\leq \gamma\rho(\Pi_\Phi P^\pi) + \kappa\|(I - \eta\Phi^\top D\Phi)^K(I - \gamma(\Phi^\top D\Phi)^{-1}\Phi^\top DP^\pi\Phi)\| \\
&\leq \gamma\rho(\Pi_\Phi P^\pi) + C\|(I - \eta\Phi^\top D\Phi)\|^K.
\end{aligned}$$

where $C = \kappa\|I - \gamma(\Phi^\top D\Phi)^{-1}\Phi^\top DP^\pi\Phi)\|$ for κ the condition number of the eigenvector matrix of $\Pi_\Phi P$.

So we can take

$$K > \frac{\log\frac{C}{1-\gamma\rho(\Pi_\Phi P^\pi)}}{\log\frac{1}{\|(I-\eta\Phi^\top D\Phi)\|}}$$

which ensures the spectral radius of TD-TN is < 1.

B.3 Proof for TD-FR, Proposition 3.2

Let us consider the case where parametrize Q with a linear function approximation, $Q = \Phi w$, $\Phi \in \mathbb{R}^{|\mathcal{S}|\cdot|\mathcal{A}|\times p}$, $w \in \mathbb{R}^p$.

B.3.1 Part 1: Fixed point of the regularized loss

Let us look at when the gradient is 0:

$$-\Phi^\top D(R + \gamma P^\pi\Phi w - \Phi w) + \kappa\Phi^\top D\Phi(w - \bar{w}) = 0$$

Thus $\Phi^\top D(I+\kappa-\gamma P^\pi)\Phi w = \Phi^\top DR + \kappa\Phi^\top D\Phi\bar{w}$. We call

$$\boxed{w_\kappa(\bar{w}) = (\Phi^\top D(I+\kappa-\gamma P^\pi)\Phi)^{-1}(\Phi^\top DR + \kappa\Phi^\top D\Phi\bar{w})}$$

the solution of the regularized problem. We denote $A_\kappa = \Phi^\top D(I+\kappa-\gamma P^\pi)\Phi$ the regularized *iteration* matrix. The TD(0) update is therefore

$$\begin{aligned} w_{t+1} &= (I-\eta A_\kappa)w_t + \eta(\Phi^\top DR + \kappa\Phi^\top D\Phi\bar{w}) \\ &= (I-\eta A_\kappa)w_t + \eta A_\kappa w_\kappa(\bar{w}) \end{aligned}$$

Therefore

$$w_{t+1} - w_\kappa(\bar{w}) = (I-\eta A_\kappa)(w_t - w_\kappa(\bar{w})) \tag{14}$$

B.3.2 Part 2: Difference between regularized optima and true optima

Let us look at the quantity $w_\kappa(\bar{w}) - w^*$ where $w^* = A_0^{-1}\Phi^\top DR$, the solution of the unregularized problem. First, we will use the fact that $A^{-1} - B^{-1} = A^{-1}(B-A)B^{-1}$ to get

$$\begin{aligned} w_\kappa(\bar{w}) - w^* &= A_\kappa^{-1}(\Phi^\top DR + \kappa\Phi^\top D\Phi\bar{w}) - A_0^{-1}\Phi^\top DR \\ &= -\kappa A_\kappa^{-1}\Phi^\top D\Phi A_0^{-1}\Phi^\top DR + \kappa A_\kappa^{-1}\Phi^\top D\Phi\bar{w} \\ &= \kappa A_\kappa^{-1}\Phi^\top D\Phi(\bar{w} - w^*) \end{aligned}$$

Thus we have

$$w_\kappa(\bar{w}) - w^* = \kappa A_\kappa^{-1}\Phi^\top D\Phi(\bar{w} - w^*) \tag{15}$$

B.3.3 All together

$$\begin{aligned} \mathcal{T}_\kappa^T(w_t) - w^* &= \mathcal{T}_\kappa^T(w_t) - w_\kappa(w_t) + w_\kappa(w_t) - w^* \\ &= (I-\eta A_\kappa)^T(w_t - w_\kappa(w_t)) + \kappa A_\kappa^{-1}\Phi^\top D\Phi(w_t - w^*), \text{ using 14 and 15} \\ &= (I-\eta A_\kappa)^T(w_t - w^* - (w_\kappa(w_t) - w^*)) + \kappa A_\kappa^{-1}\Phi^\top D\Phi(w_t - w^*) \\ &= (I-\eta A_\kappa)^T(w_t - w^* - \kappa A_\kappa^{-1}\Phi^\top D\Phi(w_t - w^*)) + \kappa A_\kappa^{-1}\Phi^\top D\Phi(w_t - w^*), \text{ Using 15 again} \\ &= \left[(I-\eta A_\kappa)^T(I - \kappa A_\kappa^{-1}\Phi^\top D\Phi) + \kappa A_\kappa^{-1}\Phi^\top D\Phi\right](w_t - w^*) \end{aligned}$$

B.3.4 Studying $I - \eta A_\kappa$

For this, let us study the eigenvalues of A_κ, and make sure they have a positive real part. Then by choosing $\eta \leq 2\,\mathfrak{Re}(\frac{1}{\lambda_{\max}})$ the matrix will be stable.

For this, we will need, an assumption, i.e that TD(0) converges for that combination of Φ, D, P and γ.

Assumption B.3. $Sp(\Phi^\top D\Phi - \gamma\Phi^\top DP^\pi\Phi) \subset \mathbb{C}^+$

Let us call $\epsilon_\kappa = \min_{\lambda\in Sp(A_\kappa)} \mathfrak{Re}(\lambda)$.

As $\lim_{\kappa\to 0^+} A_\kappa = \Phi^\top D\Phi - \gamma\Phi^\top DP^\pi\Phi$, we have $\epsilon_0 > 0$ and by continuity of the spectrum, $\exists\delta$ so that $\forall\kappa < \delta$, $\epsilon_\kappa \geq \frac{\epsilon_0}{2} > 0$. Thus we just showed that for κ small enough the matrix A_κ was also stable.

B.3.5 Studying $\kappa A_\kappa^{-1}\Phi^\top D\Phi$

Here we just need to show that for κ small enough this matrix will be stable, i.e have a spectral radius bounded by 1. It is sufficient to notice that $A_\kappa^{-1}\Phi^\top D\Phi$ has a finite limit when $\kappa \to 0$, which is equal to $A_0^{-1}\Phi^\top D\Phi$ which is indeed bounded as $A_0 = \Phi^\top D\Phi - \gamma\Phi^\top DP^\pi\Phi$ has non-zero eigenvalues as they are $\subset \mathbb{C}^+$ as per the Assumption above.

Thus, for $\lim_{\kappa\to 0} \kappa A_\kappa^{-1}\Phi^\top D\Phi = 0$ which has a spectral radius of 0. Then again, by continuity of the spectrum thus spectral radius, for κ small enough, $\kappa A_\kappa^{-1}\Phi^\top D\Phi$ has a spectral radius < 1.

Corollary B.4 (Stability of TD-FR and TD-TN)**.** *When $p = 1$, for T large enough, the convergence domain of TD-TN is included in the one of FR-TN.*

B.4 Proof for Corollary B.4

We first need to show that $Sp(\Phi^\top D\Phi - \gamma\Phi^\top DP^\pi\Phi) \subset \mathbb{C}^+$ implies that $\rho\big((\Phi^\top D\Phi)^{-1}\Phi^\top DP^\pi\Phi)\big) < \frac{1}{\gamma}$.

Let us consider $\mathbf{v}$ a eigenvector of $(\Phi^\top D\Phi)^{-1}\Phi^\top DP^\pi\Phi$ associated with the eigenvalue λ. Thus

$$\Phi^\top DP^\pi\Phi\mathbf{v} = \lambda\Phi^\top D\Phi\mathbf{v}$$

From this we multiply by γ and substract and add $\Phi^\top D\Phi\mathbf{v}$:

$$\big(\Phi^\top D\Phi - \gamma\Phi^\top DP^\pi\Phi\big)\mathbf{v} = (1-\lambda\gamma)\Phi^\top D\Phi\mathbf{v}$$

Multiplying by $\mathbf{v}^\top$:

$$\mathbf{v}^\top\big(\Phi^\top D\Phi - \gamma\Phi^\top DP^\pi\Phi\big)\mathbf{v} = (1-\lambda\gamma)\mathbf{v}^\top\Phi^\top D\Phi\mathbf{v}$$

As $\Phi^\top D\Phi$ is positive definite (non-singular by assumption), $\mathbf{v}^\top\Phi^\top D\Phi\mathbf{v} > 0$. However we can't conclude anything in the general case with non-symmetric matrices. When $p = 1$, these matrix products become real scalars as all the coefficients are real. So for $x^2 = \Phi^\top D\Phi$

$$\big(\Phi^\top D\Phi - \gamma\Phi^\top DP^\pi\Phi\big) = (1-\lambda\gamma)x^2$$

so $\big(\Phi^\top D\Phi - \gamma\Phi^\top DP^\pi\Phi\big) > 0$ implies that $(1-\lambda\gamma) > 0$, thus $\lambda < \frac{1}{\gamma}$ the maximum and only eigenvalue, thus the spectral radius of $(\Phi^\top D\Phi)^{-1}\Phi^\top DP^\pi\Phi$ is smaller than $\frac{1}{\gamma}$.

We denote by $\mathcal{D}_{\text{TD}} = \{\Phi, D | Sp(\Phi^\top D\Phi - \gamma\Phi^\top DP^\pi\Phi) \subset \mathbb{C}^+\}$ and $\mathcal{D}_{\text{TN}} = \{\Phi, D | \rho\big((\Phi^\top D\Phi)^{-1}\Phi^\top DP^\pi\Phi)\big) < \frac{1}{\gamma}\}$ the convergence domains of TD and TN ($T = +\infty$). We just proved for $p = 1$ that $\mathcal{D}_{\text{TN}} \subset \mathcal{D}_{\text{TD}}$. We know from Proposition B.2 and 3.2 that for κ small enough, FR(T) and TN(T) (FR and TN using a period update of T) and $\mathcal{D}_{\text{FR(T)}}$, $\mathcal{D}_{\text{TN(T)}}$ their convergence domains that $\lim_{T\to+\infty}\mathcal{D}_{\text{FR(T)}} = \mathcal{D}_{\text{TD}}$ and $\lim_{T\to+\infty}\mathcal{D}_{\text{TN(T)}} = \mathcal{D}_{\text{TN}}$. Thus by taking the limit we have the inclusion we needed.

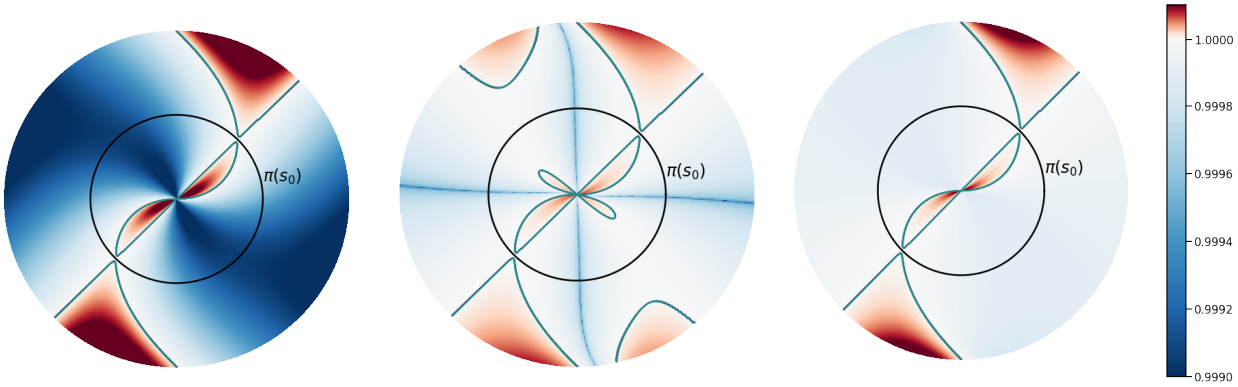

(a) **TD(0)** (b) **TN** (c) **FR**

Figure 3: **2-state MDP.** $\gamma = 0.9995$

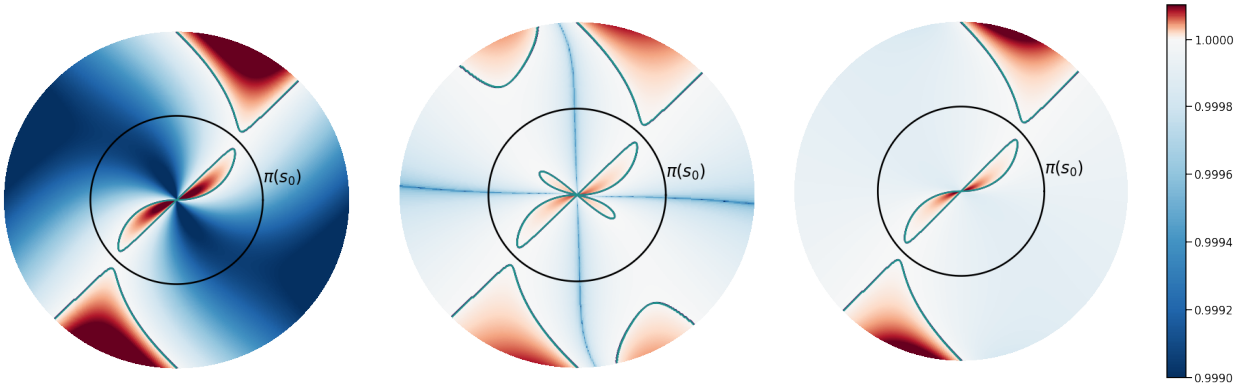

(a) **TD(0)** (b) **TN** (c) **FR**

Figure 4: **2-state MDP.** $\gamma = 0.995$

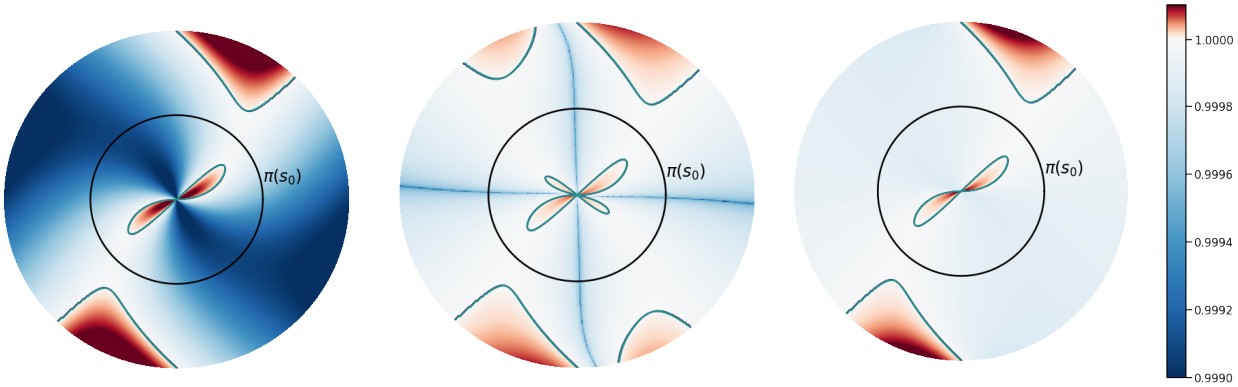

(a) **TD(0)** (b) **TN** (c) **FR**

Figure 5: **2-state MDP.** $\gamma = 0.95$

C Additional Results and Hyper-parameters

C.1 2-state MDP

We see on Appendix C.1 that increasing the discount factor leads to larger divergence regions. However, the circle of radius $\pi(s_0)$ which corresponds to the on-policy algorithm stays in the convergent domain as predicted by theory.

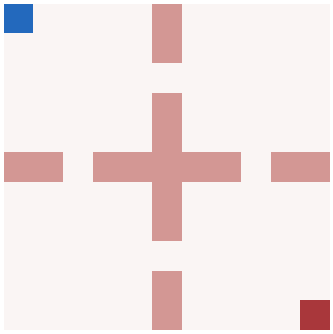

Figure 6: **4 Rooms environment.** The agent starting position is denoted in red and the goal in blue.

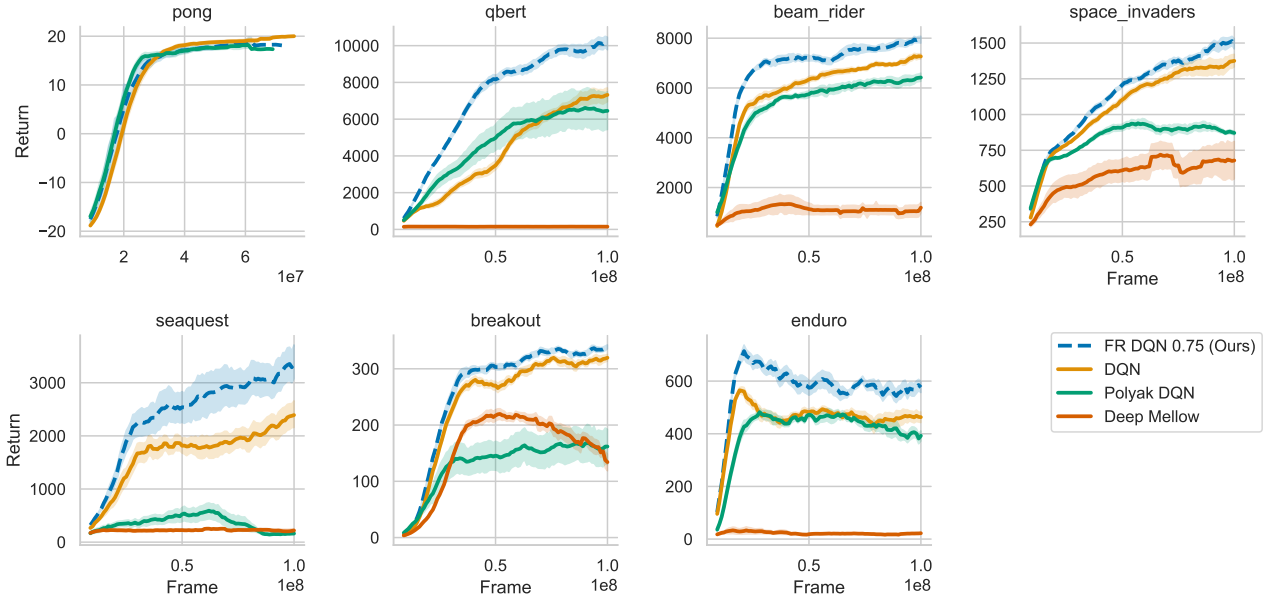

Figure 7: **DQN Atari Comparison**. Performance curves for the subset of Atari games from Mnih et al. (2013). The returns are averaged over 10 trials using the ϵ-greedy policy with $\epsilon = 0.05$.

C.2 Four Rooms

Table 2: Four Rooms Hyper-parameters

Hyperparameter	Value
learning rate	1e-4
optimizer	adam (Kingma and Ba, 2014)
discount factor γ	0.99
DNN layers	[128, 128, 4]
dimension	11×11

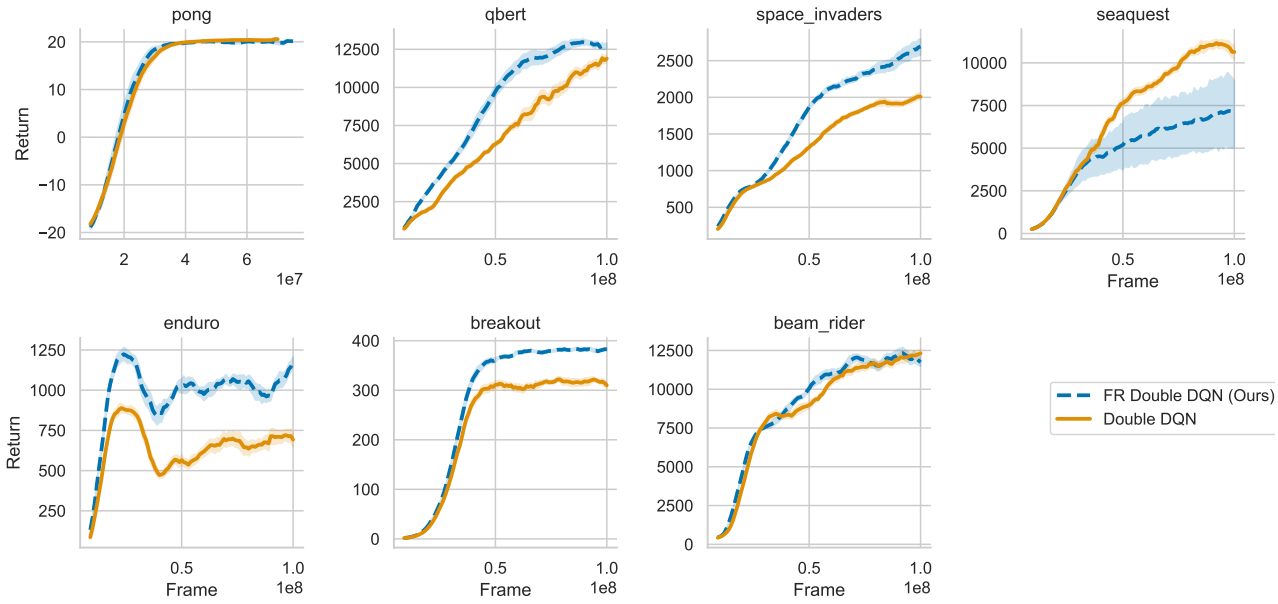

Figure 8: **Double DQN Atari Comparison**. Performance curves for the subset of Atari games from Mnih et al. (Mnih et al., 2013).

C.3 Atari

Most of the hyper-parameters have been kept from the defaut DQN and Double DQN respectively. Here is a list of the tuning that has been performed and the resulting best hyper-parameters.

Table 3: Atari Hyper-parameters

Hyperparameter	Polyak DQN	FR DQN	FR Double DQN	Deep Mellow	FR Rainbow
τ	5e-5, 2.5e-5, **1e-5**, 5e-6	-	-	-	-
TN Update Period	100	-	-	-	-
FR Update Period	-	4e4	4e4	-	3.2e4
κ	-	0.25, 0.5, **0.75**	**0.75**	-	0.25, 0.5, 0.75, 1, **2.5**, 5
Mellow Temperature	-	-	-	**25**, 50, 75, 100	-

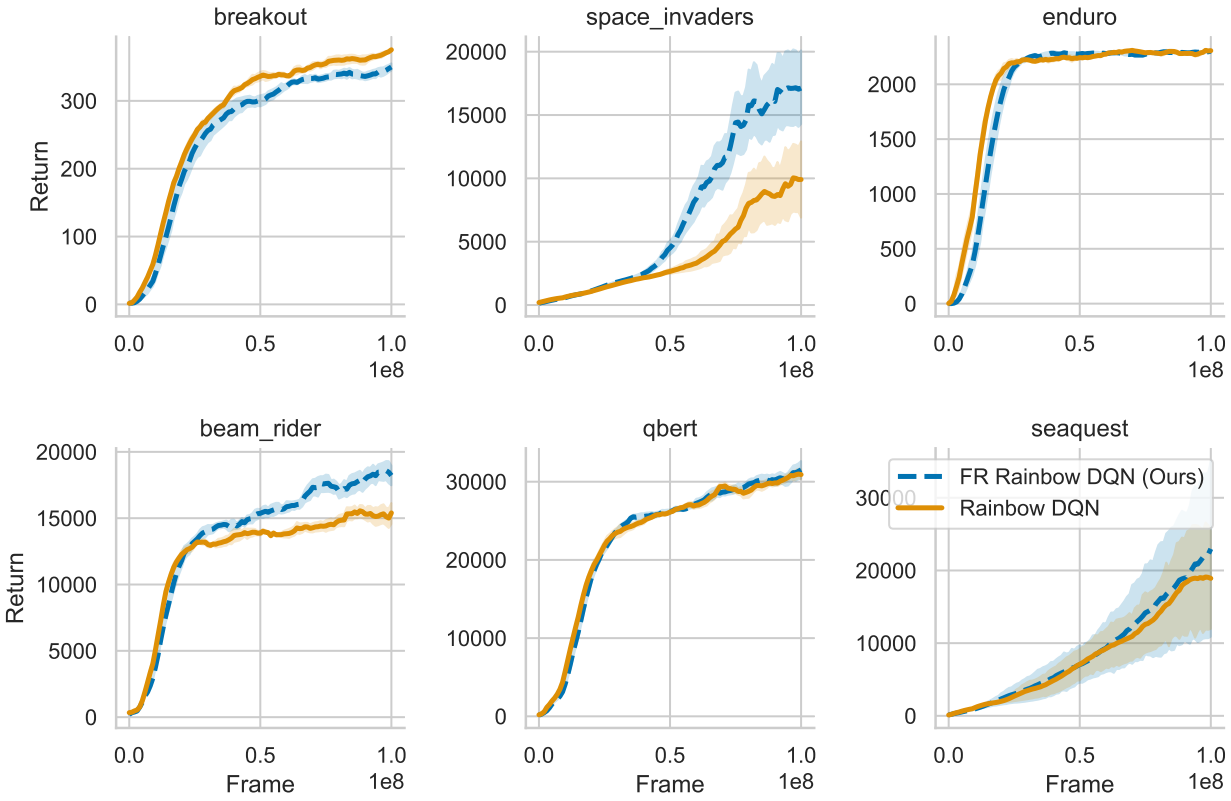

Figure 9: **Rainbow DQN Atari Comparison**. Performance curves for the subset of Atari games from Mnih et al. (Mnih et al., 2013).